

Determining the Active Surface Area for Various Platinum Electrodes

Dong Chen · Qian Tao · Ling Wen Liao ·
Shao Xiong Liu · Yan Xia Chen · Shen Ye

Published online: 17 May 2011
© Springer 2011

Abstract Various methods, i.e., the adsorption/stripping of adsorbed probe species, such as hydrogen (H), copper (Cu), and carbon monoxide (CO), oxygen and hydroxide (O/OH), potentiostatic CO/H displacement as well as double layer capacitance are exploited to evaluate the electrochemically active surface areas (ECAs) of platinum (Pt) foils, chemically deposited Pt thin film, and carbon-supported Pt nanoparticle electrodes. For the relatively smooth Pt electrodes (roughness factor < 3), the measurements from the stripping of H, Cu, and CO adlayers and CO/H displacement at 0.08 V (vs. RHE) give similar ECAs. With the increase of the surface roughness, it was found that the ECAs deduced from the different methods have the order of CO/H displacement less than the stripping of under potential deposition (UPD) Cu monolayer less than the stripping of the UPD-H adlayer. Possible origins for the discrepancies as well as the applicability of all the above-mentioned methods for determining ECAs of various Pt electrodes are discussed, and the UPD-Cu method is found to be the most appropriate technique for the determination of ECAs of Pt electrodes with high roughness factors or composed of nanoparticles with high dispersion.

Keywords Pt electrocatalysts · Electrochemically active surface areas (ECAs) · Under potential deposition (UPD) · Voltammetric stripping · Adsorbed hydrogen (H) · UPD-Cu · CO displacement method · CO adsorption

D. Chen · Q. Tao · L. W. Liao · S. X. Liu · Y. X. Chen (✉)
Department of Chemical Physics,
Hefei National Laboratory for Physical Sciences at Microscale,
University of Science and Technology of China,
Hefei 230026, China
e-mail: yachen@ustc.edu.cn

S. Ye
Catalysis Research Center, Hokkaido University,
Sapporo 001–0021, Japan

Introduction

Platinum (Pt) is one of the most active metal catalysts toward many electrochemical reactions, such as the anodic oxidation of small organic molecules and the cathodic reduction of oxygen (O₂) in proton exchange membrane fuel cells (PEMFCs) [1–3]. In practical cases, highly dispersed Pt catalysts with large surface areas are extremely important to increase the electrocatalytic reactivity [2–4]. The information on the electrochemically active surface area (ECA) of such Pt-based electrocatalysts is essential to derive the specific activity for evaluation and comparison of the different catalysts from various sources [4–9]. This is one of the prerequisites to understand the relationship between the catalytic activity and their structure/composition, which are the basis for rational design of highly efficient electrocatalysts for PEMFCs and other electrochemical processes.

The charge densities involved in the electro-adsorption (deposition) and electro-desorption (stripping) of probe species such as hydrogen (H) [5, 8, 10], copper (Cu), silver (Ag) [8, 11, 12], carbon monoxide (CO) [9], oxygen (O), and hydroxide (OH) [5], are used to estimate the electrochemically active surface areas (ECAs) of various Pt electrocatalysts, including single crystalline and polycrystalline Pt electrodes as well as carbon-supported Pt nanoparticle electrodes [8, 9]. This approach is mainly carried out by cyclic voltammetry (CV) based on a number of assumptions: (1) a saturated adlayer of the probe species is formed in a certain potential region; (2) the stoichiometric ratio between adsorbed species and surface Pt atom is a constant (for example, the ratio for Pt and H is normally assumed to be 1:1 while that for Pt and CO is 1:x, where $x=0.65$ to 0.8 depending on the research groups) [9, 13–16]. Among these processes, the under potential deposition (UPD) processes of H and some metal cations on Pt

electrode surfaces are commonly employed. By controlling the negative limit of the potential sweep slightly positive than the equilibrium potential (E_{eq}) required for bulk deposition, one is able to control the coverage of the adatoms at the electrode surface in mono- or sub-monolayer quantities with a defined structure and thus to estimate the ECAs from the charge passed in the UPD or the subsequent stripping processes [17, 18].

Recently, Watt-Smith et al. determined the ECAs of Pt/C catalysts used in PEMFC from the charge densities involved in the UPD processes of H and Ag [8]. They reported that a variation in the ECAs between these two methods is up to ca. 100% for a high-loaded sample whilst the difference is ca. 30% for a low-loaded sample. They claimed that it is quite critical to control the Ag^+ concentration and deposition time for the UPD-Ag process on these highly dispersed Pt electrode surfaces to get a reliable charge to evaluate the surface area [8]. It is suggested that after a certain deposition time, the deposition of silver no longer occurs as a monolayer, instead, silver will further deposit onto the first silver layer. Recently, Lindstrom et al. investigated temperature and humidity effects on the ECA of the carbon-supported Pt catalyst in the PEMFCs using in situ CV and reported that the charges of the CO stripping are essentially independent of temperature, but that of the UPD-H decrease with temperature due to the significant overlap with the current from the hydrogen evolution reaction (HER) [9]. On the other hand, they found that both charges from the UPD-H and CO stripping decrease with humidity in the fuel cell [9]. Based on these results, they proposed that CO stripping is more accurate for measuring the ECAs of the electrocatalysts in a fuel cell. All these results illustrate that systematic and quantitative assessment of the possible errors associated with the commonly used methods for ECA determination is highly demanding for accurately evaluating the actual ECA of Pt-based electrocatalysts and the utility of complex, porous fuel cell electrodes.

In fact, some of the problems have been pointed out qualitatively in the literature [4–6]. For example, the stripping of UPD-H is a widely used approach for evaluating the ECA of Pt-based electrocatalysts [8, 9, 19, 20]. From the studies using Pt single crystalline electrodes, it is confirmed that the charge in the UPD-H region is strongly affected by surface orientation and anion co-adsorption. It is proposed that different ensemble sites are necessary for UPD-H formation at different single crystalline faces [21–24]. Jerkiewicz pointed out that due to the variable distribution of domains with different orientations and its ratio to the corner and edge atoms as well as the presence of various defect sites on the practical catalysts surfaces, the charge density for stripping of saturated UPD-H layer may not be a fixed constant [6]. However, these

methods are still used without carefully taking such factors into accounts which may have lead to misleading results in the comparison of different electrocatalysts.

In this contribution, we present a systematic and quantitative analysis of different methods used for the determination of the ECAs of Pt-based electrocatalysts. The charge densities associated with UPD-H, UPD-Cu, and CO/H displacement have been exploited to evaluate the ECAs of various Pt electrodes, i.e., polycrystalline Pt electrodes with different roughness factors (RF), Pt thin films chemically deposited onto a silicon (Si) surface, and electrodes composed of Pt nanoparticles (Pt/Vulcan from E-tek) attached to glassy carbon (GC) electrodes with different loadings. These electrodes are typical the ones used in fundamental and practical research. For example, the Pt thin film electrodes deposited on Si surface are used as a working electrode for the mechanistic and kinetic studies of the electrocatalytic oxidation of small organic molecules by electrochemical in situ infrared spectroscopy under attenuated total reflection configuration (ATR-FTIRS) [25–29]. We found that the ECAs determined from the charge densities associated with UPD-H, UPD-Cu, and CO/H displacement are comparable for the Pt electrodes with low roughness ($RF < 3$). However, for the Pt electrodes with higher roughness and particle dispersion, the ECAs determined by UPD-H are usually higher than UPD-Cu and CO/H displacement. Other methods such as CO stripping, PtOH/PtO_x adsorption and double layer charging capacitance have also been briefly discussed.

Experimental

Pt foils (Tian Jin Aida Corp.) were firstly polished with Al₂O₃ powders down to 0.5 μm, and then ultrasonically cleaned in Milli-Q water and acetone three times each. After that, a Pt foil was annealed by a butane flame to red for several seconds before installing into the cell (denoted as Pc-Pt-I hereafter). Another Pt foil was directly etched in aqua regia for 1 h to roughen the electrode surface and was then cleaned thoroughly with Milli-Q water (denoted as pc-Pt-II). The Pt thin-film electrode with a thickness of ca. 100 nm is chemically deposited onto the flat reflecting face of a hemicylindrical Si prism which was catalyzed by the preformed Pd nuclei according to a procedure described in ref. [25]. Working electrodes composed of Pt nanoparticles (20% wt. Pt/Vulcan from E-tek) attached to glassy carbon electrode with two different loadings of 30 and 60 μg/cm² were denoted as nano-Pt-I and nano-Pt-II, respectively. The details for the preparation procedures for the nano-Pt electrodes have been given in ref. [30]. The geometric area of the Pt foil and Pt thin-film electrodes exposed to electrolyte solution in the cell is ca. 1.0 cm², while that for nano-Pt electrodes is ca. 0.28 cm².

The thin layer flow cell (cell volume of ca. 15 μl) used in this study is described in detail in ref. [28]. Pt foil and a reversible hydrogen electrode (RHE) were used as counter and reference electrodes, respectively. All the potentials in this study are given with respect to RHE. The electrolyte flow rate was controlled by hydrodynamic pressure and a flow rate controller at the outlet. The composition of the electrolyte flowing through the cell can be easily changed by switching between different electrolyte supplying bottles under potential control. The electrolyte solution was flowed continuously through the cell with a flow rate of 4 ml/min, i.e., the electrolyte solution in the flow cell is expected to be replaced ca. four times per second.

Electrode potential was controlled by a potentiostat (CHI400a, Shanghai Chenghua, China). All the experiments were carried out at room temperature. Millipore Milli-Q water ($18.2 \text{ M}\Omega \text{ cm}^{-1}$), sulfuric and perchloric acid (GR grade, from Sinopharm), CuSO_4 (AR grade, from Sinopharm) were used to prepare the solutions. The supporting electrolyte used in all measurements in this study was 0.5 M H_2SO_4 or 0.1 M HClO_4 and was constantly purged by N_2 (99.999%, Nanjing Special Gas Corp.). Before the measurement, continuous potential cycles in the potential region from 0.05 to 1.3 V at a scan rate of 50 mV/s in 0.5 M H_2SO_4 were carried out to clean the Pt foil or Pt thin-film electrode surfaces until the reproducible CV was obtained. UPD-Cu was carried out in 0.5 M H_2SO_4 +1 mM CuSO_4 . CO (99.95%, Nanjing Special Gas Corp.) was used for the CO displacement or CO adsorption/stripping measurement after holding the electrode potential at 0.08 V or other constant potentials in the supporting electrolyte. All the data were averaged over three sets of measurements.

Results

Determination of the ECA by Stripping of UPD-H Monolayer

Figure 1 shows typical CVs (solid lines, 0.05–1.30 V, sweep rate of 20 mV/s) on (a) pc-Pt-I and (b) pc-Pt-II recorded in 0.5 M H_2SO_4 . The general shape for these two electrodes is nearly the same, except that the amplitude of the current for pc-Pt-II is higher than that for the pc-Pt-I at the same potential. The adsorption and desorption waves for UPD-H are observed between 0.05 and 0.4 V. Two pairs of redox peaks are observed at 0.27 and 0.12 V, which are attributed to strongly and weakly adsorbed H atoms at the Pt surfaces with (100) and (110) orientations [10, 21, 22], respectively. A flat current region (so-called double-layer region) is observed from 0.40 to 0.75 V. With a further positive shift in electrode potential, an oxidation wave appears at $E > 0.85$ V, and a reduction peak appears around

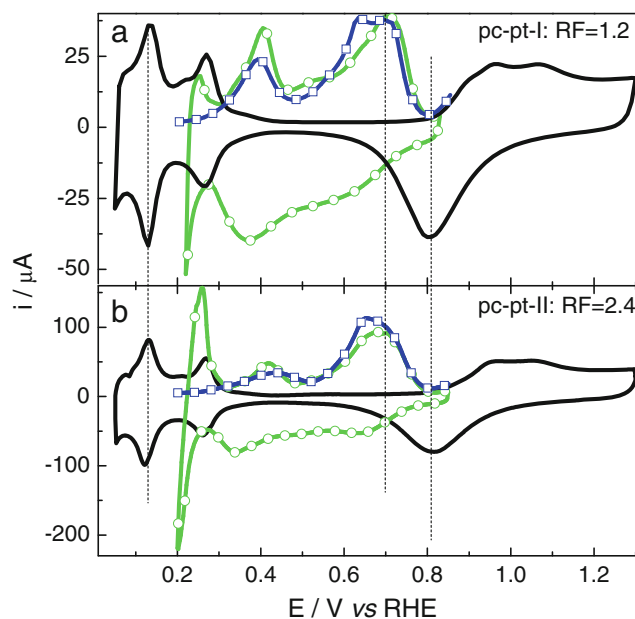


Fig. 1 CVs of a pc-Pt-I and b pc-Pt-II electrodes in 0.5 M H_2SO_4 (solid line, 0.05–1.3 V), 0.5 M H_2SO_4 +1 mM CuSO_4 (line with circle, 0.20–0.85 V), and in 0.5 M H_2SO_4 after holding at 0.245 V for 300 s in 0.5 M H_2SO_4 +1 mM CuSO_4 (line with square, 0.20–0.85 V); scan rate=20 mV/s

0.8 V in the subsequent negative-going sweep. This pair of redox peak is attributed to the formation and reduction of Pt hydroxide/oxide (PtOH/PtO_x) at the Pt electrode surface. All these features are similar to those reported in the literature [31–33].

Figure 2 displays a typical CV (solid line) of the Pt thin film chemically deposited on a Si surface under similar conditions. The features of the CV are generally similar to those of the Pt foils (Fig. 1) while the peaks at 0.28 and 0.13 V are less sharper, which may be due to the rough nature of the chemically deposited Pt thin-film surface which contains domains with various orientations. Figure 3 shows typical CVs (solid line) of 20% wt. Pt nanoparticles supported on Vulcan 72 attached to a GC electrode with loadings of (a) $30 \mu\text{g}/\text{cm}^2$ (nano-Pt-I) and (b) $60 \mu\text{g}/\text{cm}^2$ (nano-Pt-II) recorded in 0.5 M H_2SO_4 under similar conditions. From Fig. 3 it is seen that the peak height and peak area for UPD-H increase with Pt loading. Compared to the Pt thin-film electrode (Fig. 2), the peaks for the UPD-H and surface oxide formation/reduction on the nano-Pt electrodes become even broader. Furthermore, it is found that for both the Pt thin-film and nano-Pt electrodes the peak height and peak area in negative-going sweep are always higher than those in the positive-going sweep. Similar issues have also been observed by other groups, and its reason is not clear at the present stage [8, 9, 34].

In the present work, the charge determined from the stripping process of the adsorbed UPD-H monolayer on

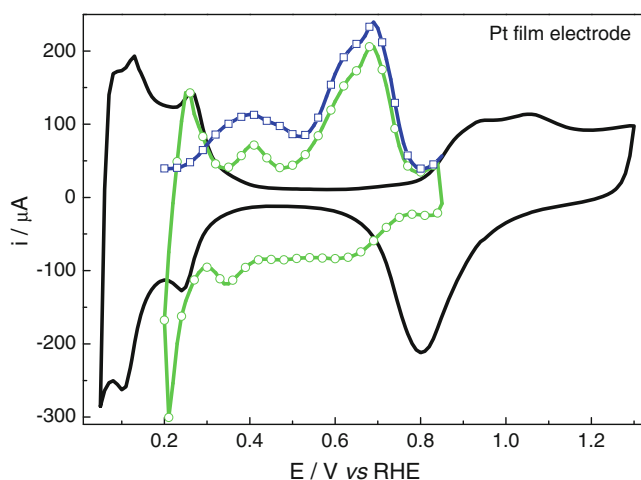


Fig. 2 CVs of a chemically deposited Pt thin-film electrode in **a** 0.5 M H_2SO_4 (solid line, 0.05–1.3 V), **b** 0.5 M H_2SO_4 +1 mM CuSO_4 (line with circle, 0.20–0.85 V), and **c** 0.5 M H_2SO_4 +1 mM CuSO_4 after holding at 0.245 V for 300 s (line with square, 0.20–0.85 V); scan rate=20 mV/s

the Pt electrode (Q_{H}) is adopted to estimate the ECAs for all these Pt electrode surfaces. The negative limit for the formation of a monolayer of UPD-H atoms at Pt electrodes in 0.5 M H_2SO_4 or 0.1 M HClO_4 is assumed to be 0.05 V as usual [4, 10, 35]. If we know the charge density (Q_{S} , in unit of microcoulomb per square centimeter) for the stripping of a monolayer of the UPD-H atoms on a

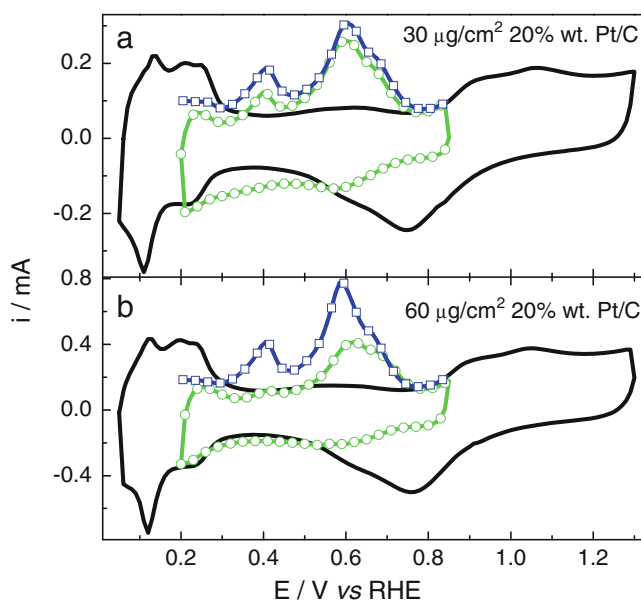


Fig. 3 CVs of nano-Pt electrodes composed of 20% wt. Pt/Vulcan nanoparticles with catalysts loading of **a** 30 $\mu\text{g}/\text{cm}^2$ and **b** 60 $\mu\text{g}/\text{cm}^2$ in 0.5 M H_2SO_4 (solid line, 0.05–1.3 V), in 0.5 M H_2SO_4 +1 mM CuSO_4 (line with circle, 0.20–0.85 V), and in 0.5 M H_2SO_4 after holding at 0.245 V for 300 s in 0.5 M H_2SO_4 +1 mM CuSO_4 (line with square, 0.20–0.85 V); scan rate=20 mV/s

reference Pt electrode with a well-defined surface structure, an ECA can be determined according to the following equation:

$$A = \frac{Q_{\text{H}}}{Q_{\text{S}}} \quad (1)$$

However, on a polycrystalline Pt electrode surface, it is difficult to get an exact value of Q_{S} for UPD-H due to the reasons mentioned in the “Introduction” section. Usually, an empirical value of 210, 220, or 230 $\mu\text{C}/\text{cm}^2$ has been suggested for Q_{S} , depending on the research groups [10, 36, 37]. The ECAs determined from the stripping process of the UPD-H monolayer are calculated according Eq. 1 and are listed in Table 1. In the present work, we found that for the smooth Pt electrodes Q_{S} of 220 $\mu\text{C}/\text{cm}^2$ gave less deviations for the ECAs results with other approaches, thus this constant is chosen in this work.

Determination of the ECA by Stripping of UPD-Cu Monolayer

Based the Nernst equation [38], equilibrium potential (E_{eq}) for Cu bulk deposition in the solution is estimated to be ca. 0.25 V in 0.5 M H_2SO_4 containing with 1 mM Cu^{2+} . From a thermodynamic point of view, it is expected that the UPD and bulk deposition (i.e., overpotential deposition, OPD) of Cu will take place on the potential region more positive and negative, respectively, than the E_{eq} . Typical CVs of UPD-Cu on Pt foils, Pt thin-film, and nano-Pt electrodes recorded in 0.5 M H_2SO_4 +1 mM CuSO_4 between 0.20 and 0.85 V (sweep rate, 20 mV/s) are displayed in Figs. 1, 2, and ~3 (line with circles). From Fig. 1, it is seen that at the Pt foil electrode the UPD-Cu takes place in a broad potential region from 0.8 V down to ca. 0.24 V (with a plateau from 0.7 to 0.4 V and a small peak at ca. 0.35 V), and at ca. $E < 0.24$ V, a bulk deposition of Cu takes place. In the subsequent positive-going potential scan, in addition to the anodic dissolution peak for the OPD-Cu around 0.2 V, the stripping of the UPD-Cu is observed in the potential region from 0.3 to 0.8 V, but the peaks are positively shifted for more than 50 mV from E_{eq} . The slight negative and positive shifts for the respective UPD-Cu and oxidative stripping of UPD-Cu adlayer indicate that a small overpotential exists for such processes, as in agreement with literature results with pc-Pt electrode [12] but in contrast to the results from single crystalline electrodes [39]. The CVs for UPD-Cu on Pt thin-film (Fig. 2) and nano-Pt (Fig. 3) electrodes are generally similar to that for Pt foil electrodes but exhibits broader peak width and different peak height ratios, which may be attributed to the increase of surface roughness of the Pt thin-film and nano-Pt electrodes.

From the CV (circle in Figs. 1, 2, and 3) we are sure that the UPD-Cu processes occur; however, it is hard to

Table 1 ECAs and nominal roughness factor of Pt foils (pc-Pt-I and pc-Pt-II), chemically deposited Pt thin-film and electrodes composed of carbon-supported Pt nanoparticles (20% wt. Pt/XC-72, nano-Pt-I:

30 $\mu\text{g}/\text{cm}^2$, and nano-Pt-II: 30 $\mu\text{g}/\text{cm}^2$) as determined by charge measurements of UPD-H, UPD-Cu, and CO/H displacement at 0.08 V

	Geometric surface area (cm^2)	Active surface area (cm^2)			Roughness factor	UPD-H/UPD-Cu factor deviation
		$\frac{Q_{\text{H,1ML}}}{220 \mu\text{C} \times \text{cm}^{-2}}$	$\frac{Q_{\text{Cu,1ML}}}{420 \mu\text{C} \times \text{cm}^{-2}}$	$\frac{Q_{\text{CO/H}_{\text{upd}}}}{152 \mu\text{C} \times \text{cm}^{-2}}$		
		pc-Pt-I	1	1.21 \pm 0.04		
pc-Pt-II	1	2.43 \pm 0.07	2.38 \pm 0.07		2.38	2%
Pt film	1	7.71 \pm 0.23	7.27 \pm 0.22	7.41 \pm 0.22	7.27	6%
nano-Pt-I	0.28	5.97 \pm 0.18	5.11 \pm 0.15	3.83 \pm 0.16	18.25	17%
nano-Pt-II	0.28	12.75 \pm 0.38	10.51 \pm 0.32		37.54	21%

The column of “UPD-H/UPD-Cu deviation” denotes the deviation of the surface area determined from the UPD-H method taking a calibration constant of 220 $\mu\text{C}/\text{cm}^2$ from that obtained using the UPD-Cu method. See text for details

determine the exact negative limit for the formation of UPD-Cu monolayer due to the facts that (1) a small overpotential is involved for the UPD process and its subsequent stripping processes and (2) the OPD-Cu process takes place immediately after the formation of UPD-Cu monolayer. As a result, the superimposition of the current peaks for both UPD and OPD processes in the CV curves can significantly affect the charge determined for the formation of UPD-Cu monolayer. To solve this problem, the following experimental procedure was exploited by taking the advantage of facile change of the electrolyte with a flow cell.

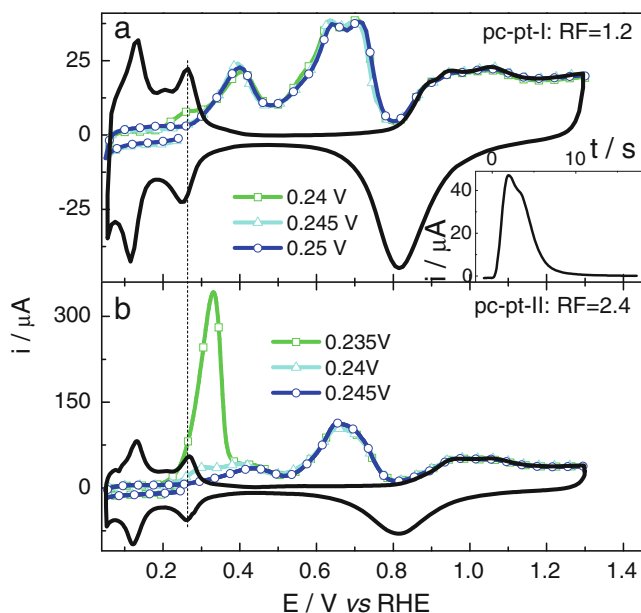


Fig. 4 Voltammetric stripping curves of UPD-Cu at **a** pc-Pt-I and **b** pc-Pt-II electrodes in 0.5 M H_2SO_4 with various negative limits (E_L) of potential sweep. The Cu adlayer is formed in 0.5 M H_2SO_4 +1 mM CuSO_4 by scanning from 0.85 V down to E_L for 300 s. The base CV (solid line) is recorded in 0.5 M H_2SO_4 for reference. Scan rate, 20 mV/s. Inset in **a** is a i - t curve at pc-Pt-I during CO/H displacement at 0.08 V after switching to CO saturated 0.5 M H_2SO_4 at ca. 0 s

The Pt electrode was firstly scanned in the potential region from 0.05 to 1.30 V in 0.5 M H_2SO_4 repeatedly to remove any possible contaminants at the electrode surface, then an electrode potential was held at 0.85 V, and the electrolyte was switched to 0.5 M H_2SO_4 +1 mM CuSO_4 . After that, the electrode potential was swept to a different negative limit of E_L near E_{eq} ($0.23 \text{ V} < E_L < 0.26 \text{ V}$, in steps of every 5 mV), and then it was kept at E_L for 5 min to ensure UPD-Cu to take place completely. Throughout the process, a continuous flow of solution (0.5 M H_2SO_4 +1 mM CuSO_4) through the cell with a rate of 4 ml/min is maintained. The purpose for using a holding time of 5 min at E_L and electrolyte flow is to exclude any possible effect from the mass transport or the surface diffusion.

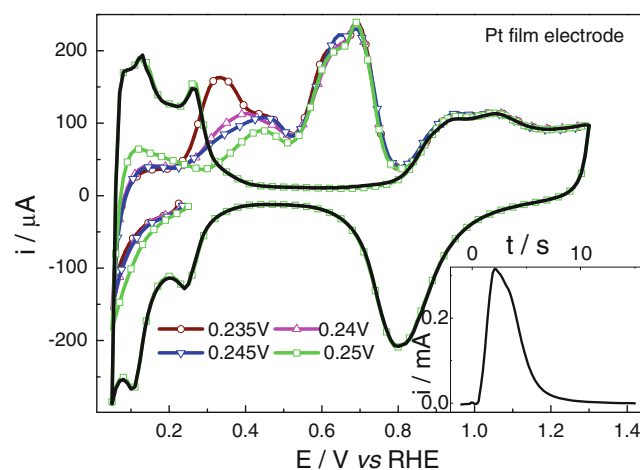


Fig. 5 Voltammetric stripping curves of UPD-Cu at a chemically deposited Pt thin-film electrode in 0.5 M H_2SO_4 with various negative limits (E_L) for Cu deposition. The Cu adlayer is formed in 0.5 M H_2SO_4 +1 mM CuSO_4 by scanning from 0.85 V down to E_L and holding at E_L for 300 s. The base CV (solid line) recorded in 0.5 M H_2SO_4 is given for reference. Scan rate, 20 mV/s. Inset: i - t curve at the Pt thin-film electrode during CO/UPD-H displacement at 0.08 V after switching to CO saturated 0.5 M H_2SO_4 at 0 s

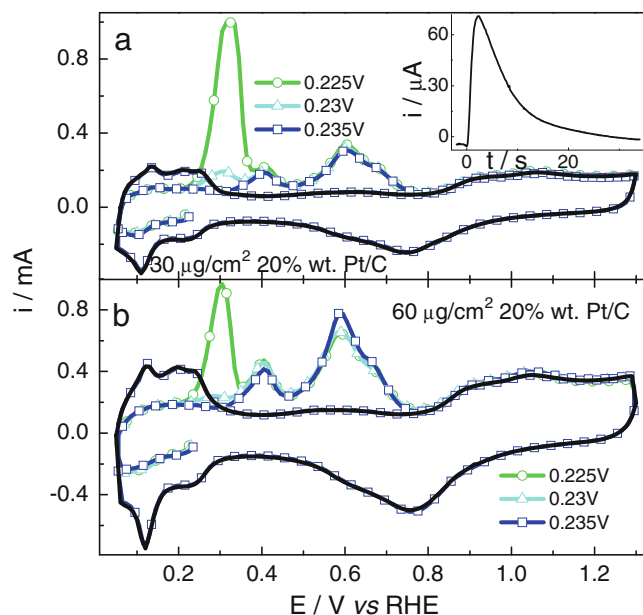


Fig. 6 Voltammetric stripping curves of UPD-Cu at 20% wt. Pt/C nanoparticle electrode with catalysts loading of **a** $30 \mu\text{g}/\text{cm}^2$ (nano-Pt-I) and **b** $60 \mu\text{g}/\text{cm}^2$ (nano-Pt-II) in $0.5 \text{ M H}_2\text{SO}_4$ with various negative limit (E_L) for Cu deposition. The Cu adlayer is formed in $0.5 \text{ M H}_2\text{SO}_4 + 1 \text{ mM CuSO}_4$ by scanning from 0.85 V down to E_L for 300 s . The base CV (solid line) is recorded in $0.5 \text{ M H}_2\text{SO}_4$ for reference. Scan rate, 20 mV/s . Inset: $i-t$ curve recorded at nano-Pt electrodes during CO/H displacement at 0.08 V after switching to CO saturated $0.5 \text{ M H}_2\text{SO}_4$ at 0 s

Then after, the electrolyte is switched back to $0.5 \text{ M H}_2\text{SO}_4$, and the inlet tubes and the cells were carefully washed when holding the electrode potential constant at E_L . After that the potential sweeping is resumed continuously down to 0.05 V at which the scan direction was reversed, and the subsequent positive scan for Cu stripping was recorded. It should be noted that the dissolution of UPD-Cu adatom is negligible when holding the electrode potential at E_L in Cu^{2+} -free solution, as is manifested by the negligible current which flows through the electrode during such processes as well as by the negligible differences in the stripping charge for UPD-Cu carried out immediately after the cleaning procedure or after waiting at E_L for 300 s or longer.

Figures 4, 5, and 6 show sets of representative CVs for the stripping process of UPD-Cu adlayer on Pt foils, Pt thin-film, and nano-Pt electrodes at a scan rate of 20 mV/s in the flow cell. From Fig. 4, it is seen that at Pt foil electrodes an additional anodic peak around 0.32 V appears only when the negative limit of the potential sweep is lower than 0.24 V , indicating that the OPD-Cu starts to occur at $E \leq 0.24 \text{ V}$. Based on the results given in Figs. 4, 5, and 6, the negative limit of the potential sweep for the formation of a monolayer of UPD-Cu on Pt foil and Pt film is found to be 0.245 V , while that for nano-Pt electrodes is ca. 10 mV more negative. It should be mentioned that we have paid great attention for the solution preparation and have

calibrated the RHE very carefully before each measurement to make sure that such small variations are not due to the small drift of RHE electrode or the pH difference of the electrolyte solution (Fig. 7).

On the other hand, it should be mentioned here that in order to get a saturated charge for UPD-Cu on the Pt electrode surfaces, a waiting time (usually longer than 300 s) at E_L is necessary for the chemically deposited Pt thin-film or highly dispersed nano-Pt electrodes. For example, it is seen that the subsequent potential cycle of Pt film electrode in $0.5 \text{ M H}_2\text{SO}_4$ in the flow cell after holding at 0.245 V for 300 s in $0.5 \text{ M H}_2\text{SO}_4 + 1 \text{ mM CuSO}_4$ shows a higher (ca. 12%) stripping charge of UPD-Cu than that observed in $0.5 \text{ M H}_2\text{SO}_4 + 1 \text{ mM CuSO}_4$ without holding at E_L for some time (Fig. 2). In fact, this tendency becomes more obvious with the increase of surface roughness (Figs. 1, 2, and 3). This indicates that more UPD-Cu adatoms are deposited on the Pt electrode surface after a period of waiting time at E_L . We have extended the waiting time at E_L up to $1,800 \text{ s}$, and no further increase in the charge for UPD-Cu is observed when the holding time is longer than 300 s for both Pt film and nano-Pt electrodes, thus we are sure that a saturated Cu adlayer is formed under this condition. On the other hand, a similar time dependence of UPD-H at constant potentials is not observed on these Pt electrode surfaces in the present study. Such a phenomenon may be related to the slow mass transport of $\text{Cu}(\text{H}_2\text{O})^{2+}$ into the inner surfaces of the rough Pt film or nano-Pt electrode or the slow diffusion of Cu adatoms along the surface after its deposition.

Therefore, the ECAs are calculated using the stripping charges for UPD-Cu after holding at E_L for 300 s in the flow cell, with an empirical value of $420 \mu\text{C}/\text{cm}^2$ for Q_S as suggested in the literature [5, 11] and after proper correction of the effects of double layer charging and H/anion adsorption (Fig. 7) The ECA values are summarized in Table 1, and the corresponding RFs are estimated based on the known geometric area. As expected from the sample preparation, RFs increase in a sequence of pc-Pt-I (1.2), pc-Pt-II (2.4), Pt thin film (7.2), nano-Pt-I (18.2), and nano-Pt-II (37.5).

Determination of the ECA by CO Displacement and CO Stripping Method

CO is known to adsorb on the Pt electrode surface strongly, and it can displace most other pre-adsorbed species such as anions and H atoms. From a series of systematic studies, Feliu and Clavilier demonstrated that the CO displacement method can be used to quantitatively analyze hydrogen and anion adsorption on the platinum single crystal electrode [40, 41]. It is found that at Pt(111) electrode the charge density for CO/H displacement at 0.08 V is ca. $152 \pm 5 \mu\text{C}/$

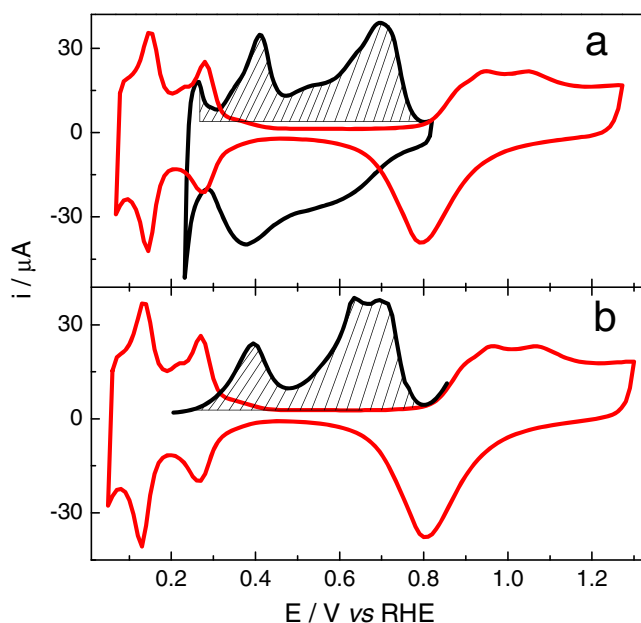


Fig. 7 A schematic illustration of the commonly used method (a) and the method used in the present study (b) for double layer correction for deriving the charge for UPD-Cu layer

cm^2 in various acid solutions even with certain amounts of anions such as HSO_4^- , Cl^- , Br^- , and $\text{C}_2\text{O}_4^{2-}$, which may adsorb on the Pt electrode surface at more positive potentials [40, 41]. In comparison with the UPD-H and UPD-Cu methods, the CO/H displacement method has a number of advantages: (1) the existence of anions in the solution does not affect the CO/UPD-H displacement charge at 0.08 V which is negative enough to avoid adsorption of most of the anions in the solution; (2) the displacement potential (0.08 V) is just positive of the onset for HER, thus an interference from the HER current is also excluded; (3) the measurement is done at constant potential, the errors associated with double layer capacitance changes is also smaller.

In the present study, the ECAs of all the Pt electrodes examined were also evaluated by measuring the charge for CO/H displacement at 0.08 V:

$$A = \frac{Q_{\text{CO/H}_{\text{UPD}}\text{at}0.08\text{V}}}{152\mu\text{C} \times \text{cm}^{-2}} \quad (2)$$

Three representative sets of $i-t$ curves recorded during CO/UPD-H displacement at 0.08 V for pc-Pt-I, Pt thin-film, and nano-Pt electrodes are given in the insets of Figs. 4, 5, and 6. From the $i-t$ curves recorded during the CO/H displacement process, it is found that the current for the oxidative removal of UPD-H first increases upon the introduction of CO containing solution, and it reaches the maximum within a few seconds, then after, it drops with time. Although, the electrolyte flow rate is largely kept the same, the time for the H oxidation current drops to ca. zero

increases with the roughness or dispersion of the catalysts in the film electrode. For Pt film, within ca. 15 s, the CO adsorption is nearly finished, while for nano-Pt electrodes, it takes more than 2 min (see Figs. 6 and 8). Such tendency is quite similar for the case with UPD-Cu process as discussed in the section “Determination of the ECA by Stripping of UPD-Cu Monolayer,” which is most probably related to mass transport resistance for CO molecules to reach the inner side of the catalyst layer. The ECAs determined according to Eq. 2 are also given in Table 1. It should be mentioned that in order to get a reliable displacement charge, in addition to allow long enough CO adsorption time, one has to pay great care in the experiment to make sure that a trace amount of O_2 has been removed from the cell system to avoid any interference from oxygen reduction reaction.

On the other hand, the stripping charge of a saturated CO adlayer has also been widely used to determine the ECAs of Pt electrodes [4, 5, 8, 9]. However, due to the facts that (1) the coverage and adsorption configuration (population of atop, bridge, and hollow sites) at Pt electrodes change with the potential and surface orientations of the Pt electrode [14, 34] and (2) the distribution of the domains with different orientations and the presence of various defect sites on the practical Pt catalysts surfaces, similar to that of UPD-H, defining a calibration constant (Q_S) for ECA determination by CO stripping is not easy. In fact, different research groups choose different saturated CO_{ad} coverage in their studies ($\theta_{\text{CO}}=0.6$ to 0.8 ML) [9, 13–16]. In the present study, we have also checked the applicability of this method. It is found that for smooth pc-Pt foil

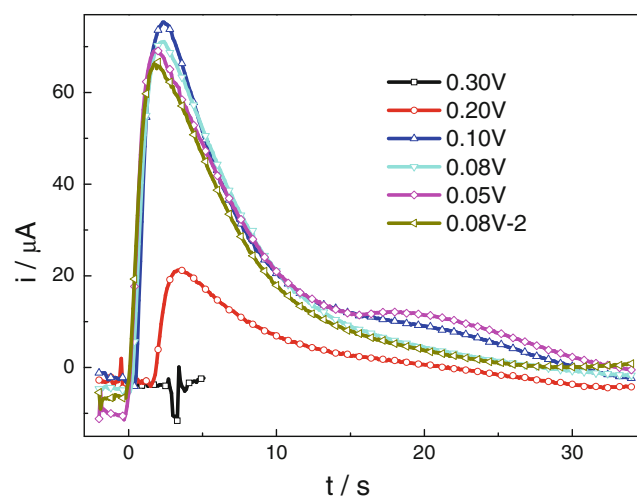


Fig. 8 $i-t$ curves for the CO adsorption on to 20% wt. Pt/C nanoparticle electrode with catalysts loading of $30 \mu\text{g}/\text{cm}^2$ (nano-Pt-I) at different various constant potentials (E_d) as indicated in the figure (the adsorption/stripping sequence is from 0.3 V down to 0.05 V and then to 0.08 V)

electrodes, the ECAs determined by the stripping charge of a saturated CO adlayer using the methods suggested by Feliu et al. [10, 14, 42] are similar to that of the UPD-Cu method under the assumptions that the saturated coverage of CO_{ad} is 0.7 ML and the charge density for the oxidation of the CO monolayer is $420 \mu\text{C}/\text{cm}^2$.

However, for chemically deposited Pt thin-film and highly dispersed nano-Pt electrodes, the ECA of the same electrode decreases with the times of the repeated CO adsorption and stripping measurements; this can be easily seen from Fig. 9, where one representative set of voltammetric curves for the oxidative stripping of a saturated CO adlayer at 20% wt. Pt/C nanoparticle electrode with a catalyst loading of $30 \mu\text{g}/\text{cm}^2$ in 0.5 M H_2SO_4 is displayed. The corresponding results from Fig. 8 and 9 are summarized in Table 2. From Fig. 9 and Table 2, it is clearly seen that after ca. four times of CO adsorption and stripping, a decrease in ca. 22% of the ECA (to the initial value) is observed. The decrease in ECA of the same electrode after the sequential CO adsorption and desorption is also evidently seen from the base CV recorded right after each measurement (Fig. 9). The ECAs for nano-Pt electrodes do not change with the repeated UPD-Cu and subsequent stripping of the Cu adlayer, this is clearly seen from Fig. 6 where the current peaks for UPD-H and Pt oxide reduction do not change after consecutive UPD-Cu and stripping. Hence, the detachment of Pt nanoparticles from the electrode surface induced by the forced electrolyte flow as well as the smoothing effect by UPD-Cu and the subsequent Cu stripping are excluded. Such continuous decrease

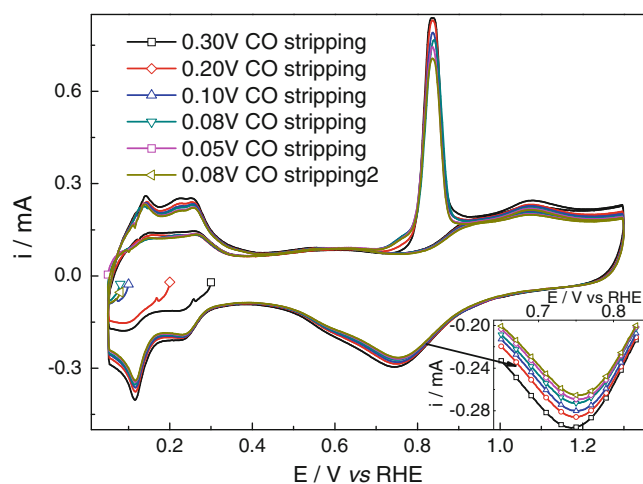


Fig. 9 Voltammetric stripping curves of saturated CO adlayers at 20% wt. Pt/C nanoparticle electrode with catalysts loading of $30 \mu\text{g}/\text{cm}^2$ in 0.5 M H_2SO_4 . The curves are measured on the same electrodes after sequential CO dosing and stripping, the CO adlayer is formed by flowing through the cell with CO saturated solution at potentials of 0.3, 0.2, 0.08, 0.05, and 0.08 V, sequentially. The inset is the magnification of the CVs in the region for Pt oxide reduction in order to help to discern different curves

in ECAs of the nano-Pt electrode with repeated CO adsorption/stripping cycles may probably be due to the CO-induced annealing of the Pt surface by smoothing the nanoparticles or the surface defects as well confirmed in the literature [43, 44].

Evaluation of Other Methods for ECA Determination

Besides these methods discussed above, we have also evaluated two other simple techniques, i.e., OH/O adsorption and double layer capacitance as suggested in the literature [5, 8, 9], in order to figure out a simple method to reasonably evaluate the ECAs of various Pt electrodes. As for measuring the charge for the formation of a monolayer of PtOH and/or PtO_x on the electrode surface in the supporting electrolyte solution by CV, unfortunately, we found that the upper limit of the CV for the formation of PtOH and PtO_x monolayer depends critically on the potential scan rate (Fig. 10 and Table 3), electrolyte composition (Fig. 10 and Table 3), as well as the surface roughness of the Pt electrode (or nanoparticle size, see Fig. 11), similar to what has been reported in the literatures [35].

The effect of electrolyte composition on the PtOH and Pt oxide formation rate can be also seen from the differences of CVs recorded in 0.1 M HClO_4 and 0.5 M H_2SO_4 as given in Fig. 10. As for the catalyst dispersion effects, it is found that the smaller the particle size, the higher the rate for the hydroxide/oxide formation on the nano-Pt surface under otherwise identical conditions (Fig. 11). Furthermore, the charge involved in the anodic scan region is always higher than that for the cathodic scan region for PtOH or PtO_x reduction, and the changes between these two cases depends largely on the catalysts structure/dispersion (inset of Fig. 11). This indicates that at a higher potential ($E > 0.8 \text{ V}$) a gradual dissolution of Pt may take place on these highly dispersed Pt catalyst surfaces. The rate for Pt oxide formation and reduction is also structure dependent. From the above analysis, we think it is hard to use the OH/O adsorption method to evaluate the ECAs especially for the practical Pt-based electrocatalysts with high roughness and dispersion.

Another commonly used method is measuring the double layer capacitance by CV. Obviously, the method cannot be applied to carbon-supported Pt electrodes since the carbon support will contribute to the capacitance. CVs in the potential region from 0.4 to 0.75 V for pc-Pt-I, pc-Pt-II, and Pt thin-film electrodes are recorded at different sweep rates from 10 to 500 mV s^{-1} and displayed in the insets of Fig. 12. Under such conditions, the double layer capacitance (C_d) can be expressed as below:

$$C_d = dQ/dE = i \cdot dt/dE = i/(dE/dt) \quad (3)$$

Table 2 The charges for CO adsorption and stripping as well as the active surface area of nano-Pt-I electrode (20% wt. Pt/XC-72, 30 $\mu\text{g}/\text{cm}^2$) at various constant potentials as calculated according to $Q_{\text{net}}^{\text{CO oxidation}} = Q_{\text{total}}^{\text{CO stripping}} - Q_{\text{ox}}^{\text{Pt}} + Q_{\text{initial}}^{\text{CO adsorption}}$ ($Q_{\text{net}}^{\text{CO oxidation}}$ is the sought-after net charge density corresponding exclusively to the faradaic oxidation of the CO adlayer. $Q_{\text{total}}^{\text{CO stripping}}$ is the charge density obtained by integration of the CO-stripping voltammogram between E_d and E_{final} . $Q_{\text{ox}}^{\text{Pt}}$ is the

charge density obtained by integration of the voltammogram of the CO-free surface between the same potential limits, and $Q_{\text{initial}}^{\text{CO adsorption}}$ is the charge density displaced at E_d by the potentiostatic adsorption of CO) [42] and assuming that the charge density for oxidation of a CO_{ad} monolayer is 420 $\mu\text{C}/\text{cm}^2$ and the saturated CO_{ad} coverage is of ca. 0.7 ML

Adsorption E/V	0.3	0.2	0.1	0.08	0.05	0.08
$Q_{\text{total}}^{\text{CO stripping}} - Q_{\text{ox}}^{\text{Pt}} / \mu\text{C}$	1,881	1,429	1,103	1,093	1,070	945
$Q_{\text{initial}}^{\text{CO adsorption}} / \mu\text{C}$	-5	234	614	567	653	518
Area (cm^2)	6.38	5.66	5.84	5.65	5.86	4.98

The original data are given in Figs. 8 and 9

where i is the current measured at various scan rates, dE/dt is the potential scan rate. From the set of CVs shown in Fig. 12, the current at 0.55 V is plotted as a function of potential scan rate and shown in Fig. 12. The slope of the linear plot in Fig. 12 gives the value of C_d for the Pt foil and Pt thin-film electrodes under examination. Taken that the real surface area of pc-Pt-I, pc-Pt-II, and Pt thin-film electrodes as determined by UPD-Cu, we found that the slopes are ca. $52 \pm 8 \mu\text{F}/\text{cm}^2$ in the potential region from 0.4 to 0.75 V for all three kinds of Pt electrodes and increases slightly with the surface roughness. The capacitance deduced in the present study is close to what is reported in the literature under otherwise identical conditions [45]. As is seen from the above values, the deviations of C_d values determined can be as high as 15%. In a word, double layer

capacity measurement can only be used for a rough evaluation of the surface area of unsupported Pt electrodes.

Discussion

Comments on UPD-H Method

The UPD-H method is the most widely used method for the determination of ECAs of monometallic Pt electrocatalysts [8, 9, 19, 20]. Jerkiewicz has pointed out that the distribution of different planes and the distribution of corner and edge atoms in the catalyst surfaces may be different and the percentage of the latter is significant, thus the charge for the formation of a saturated H adlayer at Pt electrode will change with the catalyst structure and dispersion [6]. Recently, Lindstrom et al. have also demonstrated that changing the wetting extent due to the change in cell temperature and humidity can also easily change the ECA determined by UPD-H methods [9]. In addition to the abovementioned problems, another effect exists. This will be discussed below.

Comparing the results in Table 1, it is found that for the Pt foil and thin-film electrodes the ECAs obtained by the stripping of UPD-Cu as well as CO/H displacement are quite close to that deduced from the stripping of UPD-H with a scan rate of 20 mV/s. The deviations between these three methods are below 2% for the Pt foil electrode, and it becomes slightly larger for the Pt thin-film electrode (ca. 6%). These numbers are within the range of experimental error. On the other hand, for highly dispersed nano-Pt electrodes, the ECA values determined from the three methods vary in the order that CO/H displacement at $0.08 \text{ V} < \text{UPD-Cu} < \text{UPD-H}$ under an otherwise identical condition. For the nano-Pt-I electrode, it is found that UPD-Cu can be ca. 25% higher than that for CO/H displacement (see Table 1), and the ECAs from the UPD-Cu methods can also be as large as 20% smaller than what is determined from the UPD-H method. The significant deviations

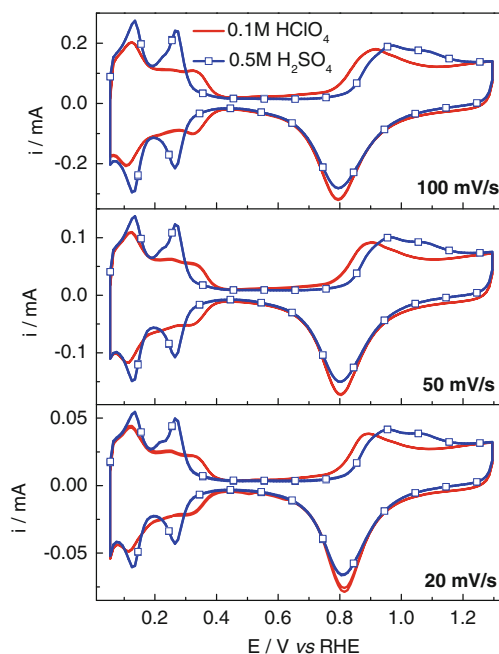
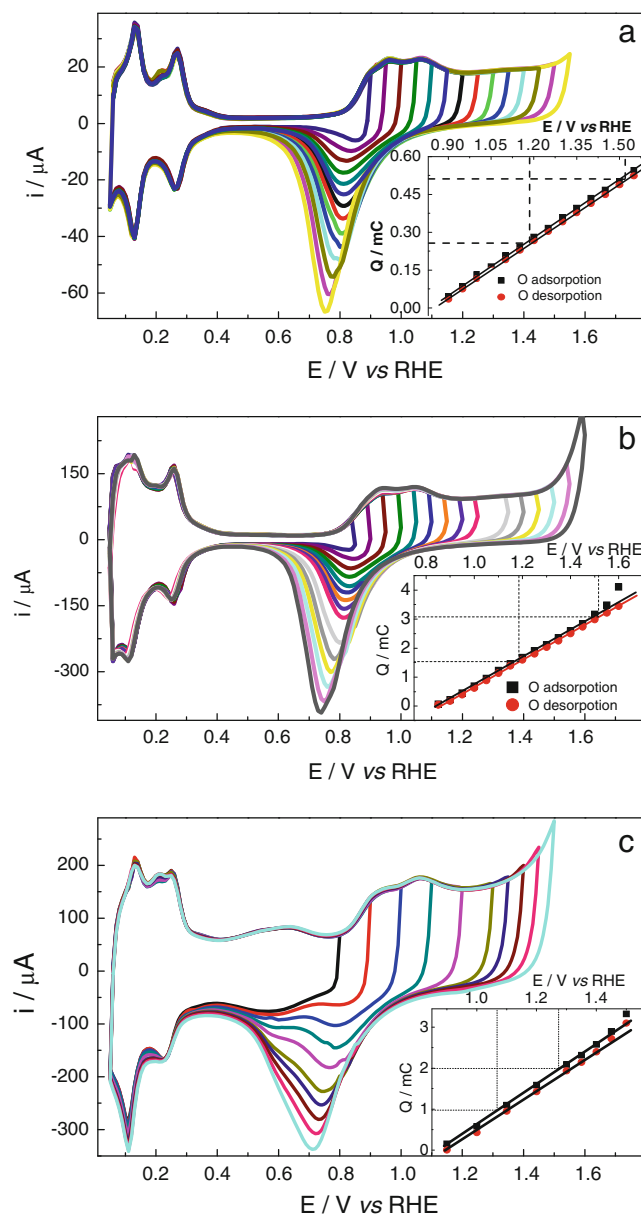


Fig. 10 CVs for pc-Pt-I electrode in 0.1 M HClO_4 (solid line) and 0.5 M H_2SO_4 (line with square) at different scan rates

Table 3 The effects of potential scan rate and electrolyte composition on the ECAs and roughness factor of pc-Pt-I electrode determined using the CVs given in Fig. 11

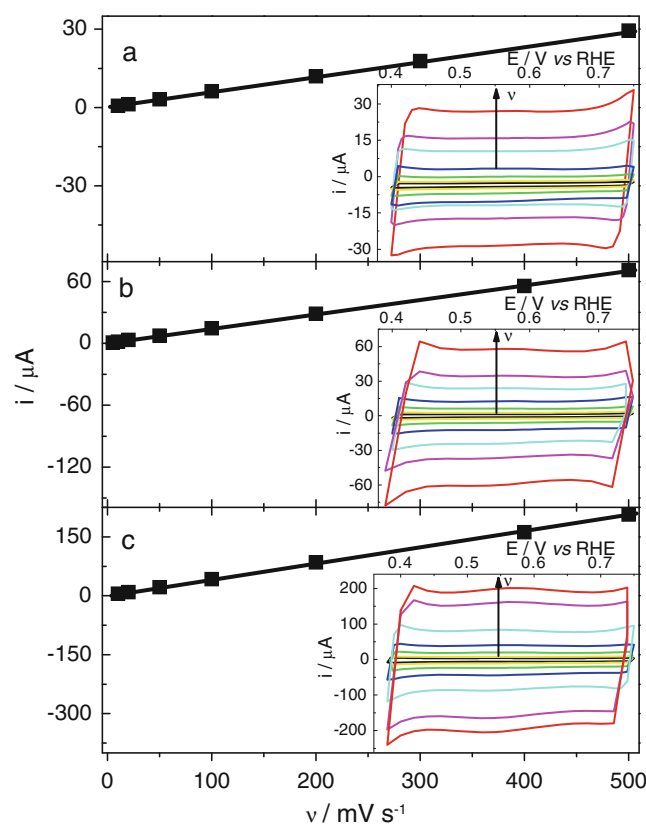
	20 mV/s		50 mV/s		100 mV/s	
	0.1 M HClO ₄	0.5 M H ₂ SO ₄	0.1 M HClO ₄	0.5 M H ₂ SO ₄	0.1 M HClO ₄	0.5 M H ₂ SO ₄
A/cm ²	1.824	2.013	1.756	1.994	1.623	1.988
Roughness factor	1.140	1.258	1.098	1.246	1.015	1.242

between the UPD-Cu and CO/H displacement methods are not clear so far, anyway due to the CO annealing problem,

**Fig. 11** CVs of pc-Pt-I, Pt film and nano-Pt-I electrodes with different positive potential limits (E_H), scan rate=20 mV/s. The insets give the charges for the oxidation of Pt and reduction of Pt oxide when scanning to different E_H

in the following, we will mainly focus on the comparison between the UPD-Cu and UPD-H method.

Comparing the results from the nano-Pt electrodes in Figs. 3, 6, and Table 1, it is found that the higher the Pt catalyst loading, the higher the deviation of the charges obtained by UPD-H and UPD-Cu methods. As shown in Table 1, in the case of Pt thin-film electrodes ($RF \approx 7$), approximately 6% of the surface sites which are accessible to H atoms cannot be used for UPD-Cu, while in nano-Pt-I ($RF \approx 18$), and nano-Pt-II electrodes ($RF \approx 38$) such differences increase to 17% and 21%, respectively. This is evident from the CVs given in Figs. 5 and 6 where an obvious UPD-H current is observed even after a saturated

**Fig. 12** Dependence of the double layer charging current at 0.55 V as a function of scan rate. Inset: a typical set of cyclic voltammograms of **a** pc-Pt-I and **b** pc-Pt-II electrodes and **c** Pt film electrode recorded in 0.5 M H₂SO₄ in the potential region from 0.35 to 0.75 V with scan rates from 10, 20, 50, 100, 200, 300 to 500 mV s⁻¹

UPD-Cu adlayer is formed or even a bulk Cu deposition occurs. A similar phenomenon is also observed after a saturated CO adlayer is formed (Fig. 9). All the results indicate that the Cu or CO adlayers cannot fully suppress the H adsorption at some sites of the rough Pt film or nano-Pt electrodes. Furthermore, we found that in Pt thin-film and nano-Pt electrodes, the ratio between the charge for UPD-H and that for the reduction of Pt oxide formed when scanning for the same higher potential limit are higher than that from Pt foils under otherwise identical conditions (Figs. 1, 2, and 3). This can be seen more clearly from Fig. 13 where the CVs for pc-Pt-I foil and Pt thin film are plotted in the same figure but with the current from Pt foil magnified by 5.4 so that for both cases the Pt oxide reduction currents are comparable.

When we just had the results for the Pt film electrode which we used intensively for the kinetic studies of the oxidation of small organic molecules with ATR-FTIRS, we have initially thought that this might be due to the fact that H may even adsorb/absorb at the Pd nuclei which are used as the seeds for Pt film growth. This possibility is excluded from the present study since a similar tendency is also observed in nano-Pt electrodes where we are sure that no Pd exists, and the deviations become even larger for the electrodes composed of highly dispersed nanoparticles. One of the possible origins for these phenomena can be related with the fact that H may adsorb at the inner surfaces (e.g., pores inside the nano-Pt electrodes) of these rough Pt thin-film electrodes at the metal surface [46]. On the other hand, these surface sites are inaccessible to other species with larger diameters such as CO, H₂O, OH/O, and Cu(H₂O)₄²⁺. Thus, the ECAs for the rough Pt electrodes obtained using these probes give smaller values. Obviously, these extra H

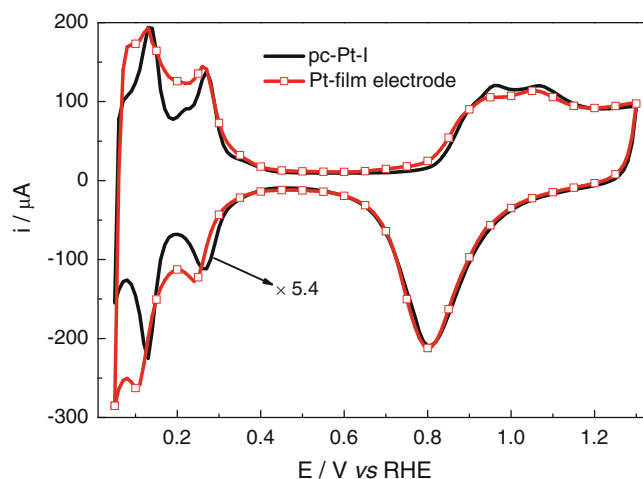


Fig. 13 CVs of pc-Pt-I (solid line) and Pt thin-film (line with square) electrodes in 0.5 M H₂SO₄ from 0.05 to 1.3 V, scan rate=20 mV/s. The current for pc-Pt-I electrode has been magnified 5.4 times to ensure that the currents in the double layer region and of the Pt oxide reduction for the two CVs are nearly superimposed on each other

adsorption sites at the inner side or inside the pores of the Pt thin-film or nano-Pt electrodes may also be inaccessible for other reactants such as the small organic molecules or gases used in PEMFCs. This suggests that the UPD-Cu, CO/H displacement, and CO adsorption/stripping methods may give lower but more accurate values for actual ECAs used in the studies on electrocatalytic reactions. However, as discussed in the section “Determination of the ECA by CO Displacement and CO Stripping Method” for the method using CO, the adsorption of CO and the subsequent stripping of CO_{ad} may cause the annealing of relatively rough electrode surfaces [43, 44].

Based on the results given above, we conclude that for determining the ECA of Pt electrodes with roughness factors below 3, these methods (i.e., UPD-H stripping, UPD-Cu stripping, and CO/H displacement) can be served with similar accuracy levels using a moderate scan rate of 20 mV/s in 0.5 M H₂SO₄ (it should be noted that scan rate and anions adsorption may cause addition deviations, Fig. 10 and Table 3), and our results demonstrated that in 0.5 M H₂SO₄, a calibration constant of 220 μC/cm² with a scan rate of 20 mV/s is more appropriate than 210 μC/cm². It should be mentioned that in the literature [4], some authors also assume that H coverage at 0.08 V corresponding to 0.77 ML, if this value is taken as a calibration constant, even for smooth Pt foil, the area determined from UPD-H method is 17% higher than that for UPD-Cu, thus this method should be discarded. Last and most importantly, for rougher Pt film or nano-Pt electrodes with high dispersion, one should be careful when using the UPD-H method to determine the ECAs; the deviations between UPD-Cu and UPD-H methods can be more than 20%. If taking the constant of 210 μC/cm² as commonly used in the literature, the deviation between UPD-Cu and UPD-H will be even larger.

Comments on the UPD-Cu Method

For relatively rough Pt thin-film or highly dispersed nano-Pt electrodes, the UPD-Cu method gives ECAs of the surface sites usual accessibility to most reactants, in contrast to the UPD-H method. Furthermore, the UPD-Cu method does not cause an appreciable annealing effect as the CO adsorption/stripping methods do. Hence, we think that the UPD-Cu method is more suitable for the determination of ECAs of the highly dispersed Pt electrode in such aspect. It should be emphasized that when using the UPD-Cu method to determine the ECAs of Pt electrocatalysts, an accurate determination of the net charge associated in the formation/stripping off of the Cu monolayer is critical. In order to reach such a target, one should pay attention to the following issues: (1) the negative limit of the potential sweep or potentiostatic deposition of Cu and the accuracy

of the reference electrode itself; (2) a holding time should be long enough to allow the Cu^{2+} to reach all the surface atoms especially those close to the inner pores which are still accessible by probing molecules; (3) to exclude charging contribution from the UPD-H and anion adsorption (see Fig. 7 on how to carry out such a correction). With a flow cell, as used in the present study, such experiments can be easily done.

However, when using a normal stationary three-electrode cell to carry out such tasks, it will be difficult to figure out the lower potential limit when a full monolayer of Cu is formed, since under such conditions: (1) one has to switch off the potential control, carefully washing the cell and then change the electrolyte; and (2) one cannot avoid partial oxidation of the Cu adlayer during such process when the potential is out of control. Another option is to use the literature results as we have reported here as the lower potential limit, then it is necessary to pay great attention to avoid any potential drift associated either with the cell through ohmic drop or due to the drift by RE, as already mentioned above. In such case, one has to use the CVs for deposition and stripping of UPD-Cu in a Cu^{2+} containing solution. Under such circumstance, we would suggest taking the background recorded in a Cu^{2+} -free solution for double layer correction (for details see Fig. 7). Obviously, the tricks discussed above are also very critical for surface area determination using the UPD method with other metals.

Conclusions

Various methods, i.e., measuring the charges for the formation or oxidative stripping of probe species such as Cu, H, OH/O, and CO, potentiostatic CO/H displacement as well as double layer capacitance have been used to determine the ECAs of Pt electrodes with various roughness and dispersion, i.e., Pt foils, chemically deposited Pt thin film, and carbon-supported Pt nanoparticles. The deviations between different methods have been analyzed quantitatively, and possible origins for such deviations have been discussed.

By assuming that the charge for the formation of a full Cu monolayer of $420 \mu\text{C}/\text{cm}^2$ and UPD-H charge of ca. $220 \mu\text{C}/\text{cm}^2$ and CO/H displacement charge at 0.08 V of ca. $152 \pm 5 \mu\text{C}/\text{cm}^2$, the ECA for relatively smooth Pt surface ($\text{RF} < 3$) derived from the stripping charge of under potential deposited Cu/H atoms or CO/H displacement are well consistent with each other.

As for rougher and highly dispersed nano-Pt electrodes, the deviation of the ECA determined using the UPD-H and UPD-Cu methods can be higher than 20%; this is explained by the H adsorption into the inner pores between the nanoparticles in the highly dispersed film electrodes, which are not accessible for Cu atoms or other species with large

diameters. The CO/H displacement and CO stripping methods are not appropriate for the determination of ECA of rough film nano-Pt with high dispersion, since adsorbed CO molecules cause a significant annealing effect (more than 20% decrease in ECAs after four consecutive times of adsorption and stripping) which changes the catalysts surface structure.

For the OH/O adsorption method, it is not possible to establish a general standard for the upper potential limit where a full monolayer of PtOH and PtO_x is formed, since Pt oxide formation/reduction depends critically on particle size and film roughness, electrolyte composition as well as electrode scan rate. The errors for the double layer capacitance can be as high as 15%.

Among all the techniques, our results reveal that for electrodes composed of highly dispersed Pt nanoparticles, ECAs obtained by the UPD-Cu method are most accurate because this method does not show appreciable annealing effects for rough Pt electrodes in contrast with the CO adsorption and stripping method, and it will not probe the surface sites which cannot be accessed by other molecules except proton as in contrast to the case of the UPD-H method. We do hope that the present quantitative estimation of errors associated with the different methods and the systematic comparisons between different approaches may invoke great attention on this issue.

Acknowledgments This work was supported by the 100 Talents Program of the Chinese Academy of Science, National Natural Science Foundation of China (NSFC) (project no. 20773116, 21073176) and the 973 Program from the Ministry of Science and Technology of China (project no. 2010CB923302).

References

1. R. Parsons, T. VanderNoot, The oxidation of small organic molecules: a survey of recent fuel cell related research. *J. Electroanal. Chem.* **257**, 9 (1988)
2. A. Hamnett, Mechanism and electrocatalysis in the direct methanol fuel cell. *Catal. Today* **38**, 445 (1997)
3. N.M. Markovic, P.N. Ross, Surface science studies of model fuel cell electrocatalysts. *Surf. Sci. Rep.* **45**, 117 (2002)
4. W. Vielstich, in *Handbook of Fuel Cells*, vol. 2, chap 21 and references cited therein, ed. by W. Vielstich, A. Lamm, H.A. Gasteiger (Wiley, Chichester, 2003)
5. S. Trasatti, O.A. Petrii, Real surface-area measurements in electrochemistry. *J. Electroanal. Chem.* **327**, 353 (1992)
6. G. Jerkiewicz, Electrochemical hydrogen adsorption and absorption. Part 1: under-potential deposition of hydrogen. *Electrocatal* **1**, 179 (2010)
7. R.W. Lindstrom, Y.E. Seidel, Z. Jusys, M. Gustavsson, B. Wickman, B. Kasemo, R.J. Behm, Electrocatalysis and transport effects on nano-structured Pt/GC electrodes. *J. Electroanal. Chem.* **644**, 90 (2010)
8. M.J. Watt-Smith, J.M. Friedrich, S.P. Rigby, T.R. Ralph, F.C. Walsh, Determination of the electrochemically active surface area of Pt/C PEM fuel cell electrodes using different adsorbates. *J. Phys. D Appl. Phys.* **41**, 174004 (2008)

9. R.W. Lindstrom, K. Kortsdotir, M. Wesselmark, A. Oyarce, C. Lagergren, G. Lindbergh, Active area determination of porous Pt electrodes used in polymer electrolyte fuel cells: temperature and humidity effect. *J. Electrochem. Soc.* **157**, 1795 (2010)
10. Q.S. Chen, J. Solla-Gullon, S.G. Sun, J.M. Feliu, The potential of zero total charge of Pt nanoparticles and polycrystalline electrodes with different surface structure. The role of anion adsorption in fundamental electrocatalysis. *Electrochim. Acta* **55**, 7982 (2010)
11. C.L. Green, A. Kucernak, Determination of the platinum and ruthenium surface areas in platinum-ruthenium alloy electrocatalysts by underpotential deposition of copper. I. Unsupported catalysts. *J. Phys. Chem. B* **106**, 1036 (2002)
12. T. Nagel, N. Bogolowski, H. Baltruschat, Towards a determination of the active surface area of polycrystalline and nanoparticle electrodes by Cu upd and CO oxidation. *J. Appl. Electrochem.* **36**, 1297 (2006)
13. K. Kinoshita, P.N. Ross, Oxide stability and chemisorption properties of supported ruthenium electrocatalysts. *J. Electroanal. Chem.* **78**, 313 (1977)
14. A. Cuesta, A. Couto, A. Rincon, M.C. Perez, A. Lopez-Cudero, C. Gutierrez, Potential dependence of the saturation CO coverage of Pt electrodes: the origin of the pre-peak in CO-stripping voltammograms. Part 3: Pt(poly). *J. Electroanal. Chem.* **586**, 184 (2006)
15. Y. Morimoto, E.B. Yeager, CO oxidation on smooth and high area Pt, Pt-Ru and Pt-Sn electrodes. *J. Electroanal. Chem.* **441**, 77 (1998)
16. T.J. Schmidt, M. Noeske, H.A. Gasteiger, R.J. Behm, P. Britz, W. Brijoux, H. Bonnemann, Electrocatalytic activity of PtRu alloy colloids for CO and CO/H₂ electrooxidation: stripping voltammetry and rotating disk measurements. *Langmuir* **13**, 2591 (1997)
17. E. Herrero, L.J. Buller, H.D. Abruna, Underpotential deposition at single crystal surfaces of Au, Pt, Ag and other materials. *Chem. Rev.* **101**, 1897 (2001)
18. E. Leiva, Recent developments in the theory of metal upd. *Electrochim. Acta* **41**, 2185 (1996)
19. M.C. Tavares, S.A.S. Machado, L.H. Mazo, Study of hydrogen evolution reaction in acid medium on Pt micro electrodes. *Electrochim. Acta* **46**, 4359 (2001)
20. Z. Jusys, R.J. Behm, Methanol oxidation on a carbon-supported Pt fuel cell catalyst - a kinetic and mechanistic study by differential electrochemical mass spectrometry. *J. Phys. Chem. B* **105**, 10874 (2001)
21. Z. Radovic-Hrapovic, G. Jerkiewicz, The temperature dependence of the cyclic-voltammetry response for the Pt(110) electrode in aqueous H₂SO₄ solution. *J. Electroanal. Chem.* **499**, 61 (2001)
22. A. Zolfaghari, G. Jerkiewicz, The temperature dependence of hydrogen and anion adsorption at a Pt(100) electrode in aqueous H₂SO₄ solution. *J. Electroanal. Chem.* **420**, 11 (1997)
23. A. Zolfaghari, G. Jerkiewicz, New findings on hydrogen and anion adsorption at a Pt(111) electrode in aqueous H₂SO₄ solution generated by temperature variation. *J. Electroanal. Chem.* **422**, 1 (1997)
24. R. Gomez, J.M. Orts, B. Alvarez-Ruiz, J.M. Feliu, Effect of temperature on hydrogen adsorption on Pt(111), Pt(110), and Pt(100) electrodes in 0.1 M HClO₄. *J. Phys. Chem. B* **108**, 228 (2004)
25. A. Miki, S. Ye, M. Osawa, Surface-enhanced IR absorption on platinum nanoparticles: an application to real-time monitoring of electrocatalytic reactions. *Chem. Commun.* **14**, 1500 (2002)
26. Y.X. Chen, A. Miki, S. Ye, H. Sakai, M. Osawa, Formate, an active intermediate for direct oxidation of methanol on Pt electrode. *J. Am. Chem. Soc.* **125**, 3680 (2003)
27. Y.X. Chen, S. Ye, M. Heinen, Z. Jusys, M. Osawa, R.J. Behm, Application of in-situ attenuated total reflection-fourier transform infrared spectroscopy for the understanding of complex reaction mechanism and kinetics: formic acid oxidation on a Pt film electrode at elevated temperatures. *J. Phys. Chem. B* **110**, 9534 (2006)
28. K. Kunimatsu, H. Uchida, M. Osawa, M. Watanabe, In situ infrared spectroscopic and electrochemical study of hydrogen electrooxidation on Pt electrode in sulfuric acid. *J. Electroanal. Chem.* **587**, 299 (2006)
29. Y.X. Chen, M. Heinen, Z. Jusys, R.J. Behm, Kinetics and mechanism of the electrooxidation of formic acid - spectroelectrochemical studies in a flow cell. *Angew. Chem. Int. Edit.* **45**, 981 (2006)
30. T.J. Schmidt, H.A. Gasteiger, G.D. Stab, P.M. Urban, D.M. Kolb, R.J. Behm, Characterization of high-surface area electrocatalysts using a rotating disk electrode configuration. *J. Electrochem. Soc.* **145**, 2354 (1998)
31. B.E. Conway, H. Angerstein-Kozłowska, W.B.A. Sharp, E.E. Criddle, Ultrapurification of water for electrochemical and surface chemical work by catalytic pyrodistillation. *Anal. Chem.* **45**, 1331 (1973)
32. T. Biegler, R. Woods, Limiting oxygen coverage on smooth platinum anodes in acid solution. *J. Electroanal. Chem.* **20**, 73 (1969)
33. G. Jerkiewicz, G. Tremiliosi-Filho, B.E. Conway, Significance of the apparent limit of anodic oxide film formation at Pt: saturation coverage by the quasi two-dimensional state. *J. Electroanal. Chem.* **334**, 359 (1992)
34. R. Gomez, J.M. Feliu, A. Aldaz, M.J. Weaver, Validity of double-layer charge-corrected voltammetry for assaying carbon monoxide coverages on ordered transition metals: comparisons with adlayer structures in electrochemical and ultrahigh vacuum environments. *Surf. Sci.* **410**, 48 (1998)
35. B.E. Conway, Electrochemical oxide film formation at noble-metals as a surface-chemical process. *Prog. Surf. Sci.* **49**, 331 (1995)
36. B.E. Conway, The electrochemical study of multiple-state adsorption in monolayers. *Acc. Chem. Res.* **14**, 49 (1981)
37. G.G. Barna, S.N. Frank, T.H. Teherani, A scan rate dependent determination of platinum areas. *J. Electrochem. Soc.* **129**, 746 (1982)
38. C.H. Hamann, A. Hamnett, W. Vielstich, *Electrochemistry* (Wiley-VCH, New York, 2007), p. 75
39. R. Gomez, H.S. Yee, G.M. Bommarito, J.M. Feliu, H.D. Abruna, Anion effects and the mechanism of Cu Upd on Pt(111) - x-ray and electrochemical studies. *Surf. Sci.* **335**, 101 (1995)
40. J.M. Orts, R. Gomez, J.M. Feliu, A. Aldaz, J. Clavilier, Potentiostatic charge displacement by exchanging adsorbed species on Pt(111) electrodes-acidic electrolytes with specific anion adsorption. *Electrochim. Acta* **39**, 1519 (1994)
41. J.M. Feliu, J.M. Orts, R. Gomez, A. Aldaz, J. Clavilier, New information on the unusual adsorption states of Pt(111) in sulfuric-acid-solutions from potentiostatic adsorbate replacement by CO. *J. Electroanal. Chem.* **372**, 265 (1994)
42. A. Lopez-Cudero, A. Cuesta, C. Gutierrez, Potential dependence of the saturation CO coverage of Pt electrodes: the origin of the pre-peak in CO-stripping voltammograms. Part 2: Pt(100). *J. Electroanal. Chem.* **586**, 204 (2006)
43. M. Arenz, K.J.J. Mayrhofer, V. Stamenkovic, B.B. Blizanac, T. Tomoyuki, P.N. Ross, N.M. Markovic, The effect of the particle size on the kinetics of CO electrooxidation on high surface area Pt catalysts. *J. Am. Chem. Soc.* **127**, 6819 (2005)
44. K.J.J. Mayrhofer, M. Hanzlik, M. Arenz, The influence of electrochemical annealing in CO saturated solution on the catalytic activity of Pt nanoparticles. *Electrochim. Acta* **54**, 5018 (2009)
45. W.G. Pell, A. Zolfaghari, B.E. Conway, Capacitance of the double-layer at polycrystalline Pt electrodes bearing a surface-oxide film. *J. Electroanal. Chem.* **532**, 13 (2002)
46. E.I. Khrushcheva, M.R. Tarasevich, Electrochemical determination of surface area of metals. *Russ. Chem. Rev.* **47**, 416 (1978)